Kinetics of Alizarin Dye Hydrolysis in Alkaline Medium for Wastewater Treatment

Badran, Ismail*+

Department of Chemistry and Earth Sciences, Qatar University, P.O. Box: 2713, Doha, QATAR

Talie, Zeinab

Department of Chemistry, An-Najah National University, P. O. Box 7, Nablus, PALESTINE

ABSTRACT: *The kinetics of the hydrolysis of Alizarin dye (ALZ) in the basic medium is investigated for the purpose of wastewater treatment. ALZ represents a group of aromatic dyes, that are heavy, toxic, and non-biodegradable. The kinetics of the reaction was followed by UV-Vis spectrophotometry and ab-initio computational methods. The effects of initial concentration, ionic strength, and temperature were studied. The kinetic salt effect (ionic strength) demonstrated that OH^- is part of the rate-determining step of the reaction. Unlike common reactions, anti-Arrhenius behavior was observed within the temperature range of 25-50°C. Therefore, the apparent activation energy was determined to be -23.91 kcal/mol. Using theoretical quantum calculations, the reaction under study was investigated using the density functionals B3LYP and B97D3, and final energies were obtained using the 2_{nd} order Møller−Plesset (MP2) theory. A complex reaction mechanism is suggested that involves the formation of an intermediate that combines the ALZ anion and water molecule attached by H-bonding. The mechanism accounted for the anti-Arrhenius behavior and the negative E_a. The standard reaction enthalpy (ΔH_{298}) obtained using the B97D3 Grimme's functional was within the range of the experimental E_a value.*

KEYWORDS: *Alizarin, Wastewater, Reaction kinetics, Negative activation energy, Anti-Arrhenius.*

INTRODUCTION

Freshwater resources are threatened by various human activities as well as climate changes [1,2]. Organic pollutants, such as synthetic dyes, pharmaceuticals, and industrial by-products, are major threats to freshwater. Such pollutants are harmful to human life and other living organisms. Therefore, there are continuing efforts to treat and reuse wastewater for irrigation and drinking purposes. Currently, there are even voices calling for a Zero Liquid Discharge (ZLD) management strategy for wastewater [3], which would not allow for any pollutants to be present in industrial effluents.

Organic dyes are one major component of wastewater contamination [4-8]. Driven by their current gigantic scale of production worldwide, dyes are responsible for one-fifth of the world's total water pollution, according to the World Bank [5]. Regrettably, industrial dye effluents are rich in hazardous chemicals, such as organic and inorganic acids, salts, coasting soda, phenols, and sulphates [9,10].

* *To whom correspondence should be addressed.*
+ *E-mail*: *ibadran@qu.edu.qa*
1021-9986/2021/5/1490-1501 12/$/6.02

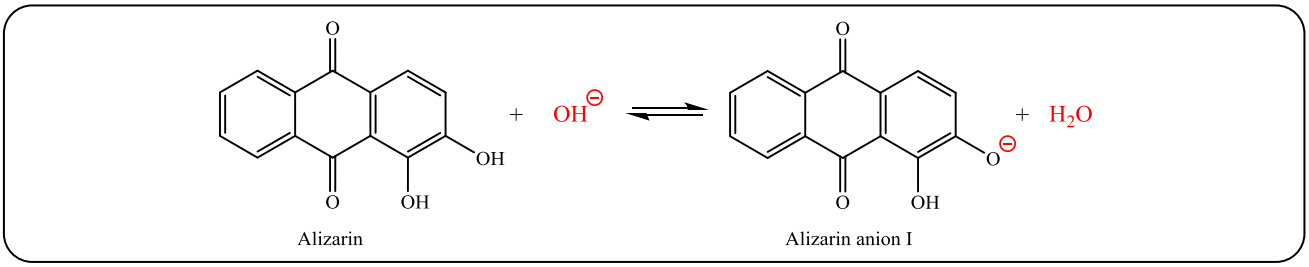

Scheme 1: Alizarin reaction with OH^- to form alizarin anion (I).

Several technologies are currently used in wastewater treatment plants to remove organic dyes. Depending on the nature and concentration of the pollutant, filtration, coagulation-flocculation, ion exchange, electrochemical treatment, advanced oxidation, or adsorption can be used. Among these technologies, adsorptive removal of dyes remains the simplest, most affordable, and most effective technology [4,8,11-17]. Undoubtedly, the success of wastewater treatment technology relies on a good balance between experimental investigation and a deep understanding of the adsorption mechanism and kinetics at the molecular level.

Recently, the removal of alizarin (ALZ) dye from an aqueous medium was investigated by our group [4]. ALZ, shown below, is reported to be very toxic, and because of its complex structure, it is non-biodegradable in an aqueous water environment [18]. Complete removal of the dye was achieved using γ-Fe_2O_3 nanoparticles as adsorbent within a short period. The adsorption was pH-dependent, and maximum removal was obtained at pH = 11. Also, the adsorption followed a Langmuir behavior, indicating a homogenous surface coverage. In addition, a thermodynamic investigation showed that the adsorption is exothermic ($\Delta H°$ = -27.8 kJ/mol) and spontaneous at room temperature ($\Delta G°$ = -6.8 kJ/mol) [4]. In order to explain the experimental findings of the ALZ adsorption on the γ-Fe_2O_3 NP surface, a sorption mechanism was suggested. As described elsewhere [4], the mechanism is initiated by the deportation of ALZ to form the alizarin anion (I), as depicted in Scheme 1.

The first deprotonation step to form anion (I) takes place in the acidic region (pKa_1 = 5.3), followed by one further deprotonation from the other OH group at a higher pH (pKa_2 = 11.5) [19]. Both anion (I) and the other dianion formed at higher pH can then interact rapidly with the Fe_2O_3 surface via hydrogen bonds [19]. In this work, we aim to investigate this mechanism further for the sake of comprehending and optimizing the conditions for ALZ's and similar dyes' adsorption on metal surfaces.

In this study, the kinetics of the hydrolysis of ALZ in the presence of OH^- was investigated experimentally. The reaction was followed by recording the absorbance of the reaction mixture in a UV-Vis spectrophotometer as a function of time. The method of initial rates was used to deduce the reaction order and the rates of the reaction under different conditions. Strangely enough, the apparent activation energy obtained during this experiment was found to be negative, indicating anti-Arrhenius behavior [20,21]. It is known that negative activation energies suggest a complex mechanism [20,22]. Such energies were recorded in many bimolecular reactions, especially those involving $OH^•$ radicals [23-25].

To account for this new finding, we performed *ab-initio* quantum theoretical calculations that aim to locate any possible transition state for the ALZ + OH^- → ALZ^- + H_2O reaction, from which, an E_a can be estimated. The theoretical study implemented both Density Functional Theory (DFT) and second-order Møller–Plesset perturbation theory (MP2) calculations.

EXPERIMENTAL SECTION

Materials

All chemicals including Alizarin dye (99.5% pure), NaOH (99% pure), and KCl (99% pure) were purchased from Sigma-Aldrich Corporation, USA, and were used as received without further purifications. Kinetic experiments Shimadzu UV-1800) coupled to a temperature controller (Fried electric device WBH-060N). Sample weighing was done using an MRC analytical balance (ASB-310-C2-V2). Ultrasonic bath sonicator (model LUC-405) was used to prepare the ALZ solutions. For the temperature study, all solutions were thermostated at the specific temperature for 30 min. prior to each kinetic run.

Kinetics experiments

2.00×10^{-5} M Alizarin stock solution was prepared by dissolving 4.80 mg ALZ (240.21g/mol) in 1000 mL distilled water and sonicated the mixture for 60 min. 0.1 M NaOH and 1.0 M KCl solutions were prepared on daily basis from their pure powders and kept covered and sealed in dark containers.

Prior to each experiment, the UV-Vis instrument was zeroed using distilled water. For a typical kinetics experiment, a clean 4.0 mL UV-Vis glass cuvette was filled by 2.5 mL of the 2.00×10^{-5} M dye solution. Then, 0.5 mL of 0.1 M NaOH was injected into the cell using a micropipette. Immediately after the injection, the solution absorbance was recorded at a constant wavelength of 560.0 nm which corresponds to λ_{max} of ALZ, up to 120 min. In order to establish the reaction order using the method of initial rates, further kinetics experiments were done by changing the volume ratio of ALZ and OH^- but keeping the total volume at 3.0 mL. Each kinetic run was repeated three times. The data were then analyzed using Origin [26].

Determination of kinetics parameters

The reaction under study can be expressed as:

$$ALZ + OH^- \rightarrow ALZ^- + H_2O \quad (1)$$

Hydrolysis of organic dyes in the basic medium can be expressed by a reaction mechanism composed of a) rapid equilibrium with a reaction intermediate and b) slow decompaction into the final product/s [21,27-29]:

$$A + B \underset{k_{-1}}{\overset{k_1}{\rightleftharpoons}} C \xrightarrow{k_2} P \quad (2)$$

For the sake of this study, the following mechanism is considered:

$$ALZ + OH^{\ominus} \underset{k_{-1}}{\overset{k_1}{\rightleftharpoons}} (II)^{\ominus} \xrightarrow[slow]{k_2} ALZ^{\ominus} + H_2O \quad (3)$$

where (II^-) is a reaction intermediate whose structure is to be discussed later in this paper.

Since the last step is the rate-determining one, the rate law is given by:

$$Rate = k_2 \left[II^- \right] \quad (4)$$

If the steady-state rate of change of intermediate II does not change over the course of the experiment:

$$\frac{d\left[II^- \right]}{dt} = k_1 [ALZ]\left[OH^- \right] - k_{-1}\left[II^- \right] - k_2\left[II^- \right] = 0$$

$$\frac{d\left[II^- \right]}{dt} = k_1 [ALZ]\left[OH^- \right] - (k_{-1} + k_2)\left[II^- \right] = 0$$

Applying the steady-state approximation:

$$k_1 [ALZ]\left[OH^- \right] = (k_{-1} + k_2)\left[II^- \right]$$

$$\left[II^- \right] = \frac{k_1 [ALZ]\left[OH^- \right]}{(k_{-1} + k_2)} \quad (5)$$

By substituting Eq. (5) in (4):

$$Rate = \frac{k_1 k_2 [ALZ]\left[OH^- \right]}{(k_{-1} + k_2)} \quad (6)$$

This equation can be simplified into:

$$Rate = k_r [ALZ]\left[OH^- \right] \quad (7)$$

Where the reduced rate is constant $k_r = \frac{k_1 k_2}{(k_{-1} + k_2)}$.

By using an excess concentration of OH^-, the equation becomes:

$$Rate = k'[ALZ] \quad (8)$$

where the apparent pseudo-first-order rate constant $k' = k_r[OH^-]$.

In this work, the method of initial rates [20,22] was used to verify the first-order kinetics of Reaction (8). The initial rate of the disappearance of ALZ can be obtained from a plot of the absorbance vs. time, followed by a least-square linear fitting of the first part of the plot, as illustrated in Fig. 1 [22,30]. This is based on the fact that the dye absorbance is in direct relationship to its concentration according to Beer-Lambert law [31].

Therefore, the reaction order can be obtained by taking the logarithms of each side of Eq. (8), giving:

$$\log(rate) = \log(k') + m \log[ALZ] \quad (9)$$

where (m) is the order of the reaction in respect to ALZ. Thus, a plot of log (rate) vs. log [ALZ] should provide a straight line with slope equals the order (m), and intercept equals log (k').

Theoretical calculations

The *ab-initio* calculations used in this work were explained in detail elsewhere [32-34]. Briefly, ALZ, its anion, and all other species were first optimized at B3LYP/6-31+G(d,p) level of theory, followed by frequency calculation at the same level. Zero-Point Energies (ZPE) were used without any scaling. In order to obtain better energies, the 2nd order Møller–Plesset perturbation theory (MP2) was used with the 6-311+G(d,p) basis set. Because the reaction of interest takes place in an aqueous medium, the B97D3 density functional suggested by Grimme, which includes solution dispersion, was also tested with the same 6-31+G(d,p) basis set [35]. Water was added to the calculations by specifying the (solvent=water) in the SCRF keyword in Gaussian. The level of theories used in this work proved to give good results for similar systems [32,34,36].

Enthalpies at zero kelvin (H_0) were calculated by adding the single point (SP) energy obtained at MP2/6-311+G(d,p) level of theory to the ZPE obtained at either B3LYP or B97D3 levels. The enthalpies 298K (ΔH_{298}) and Gibbs free energies (ΔG_{298}) were determined by adding either the enthalpy correction ($H_{corr.}$) or Gibbs free energy correction ($G_{corr.}$) to H_0. The entropies of activation ($\Delta S^{\ddagger}$) was calculated using:

$$\Delta S = \frac{\Delta G - \Delta H}{T} \qquad (10)$$

All calculations were done using Gaussian 16 [37] and viewed by Gaussview [38].

RESULTS AND DISCUSSION

Kinetics experiments

The UV-Vis spectrum of the ALZ dye used in this study exhibits a maximum of 567.5 nm. Therefore, the kinetics study was performed at this λ_{max}. The kinetics experiments were performed by filling the UV-Vis cuvette with a fixed amount of 2.00×10^{-5} M ALZ dye, followed by the injection of 0.1 M NaOH, and recording the absorbance of the reaction mixture with time. Excess concentration of NaOH was used to eliminate its effect on the rate. Therefore, the rate of the reaction depends only on the dye concentration. Fig. 2 shows a representative kinetic run with 2.0 mL of ALZ dye and 1.0 mL of the base at room temperature. As explained in the experimental section, the initial rate of the

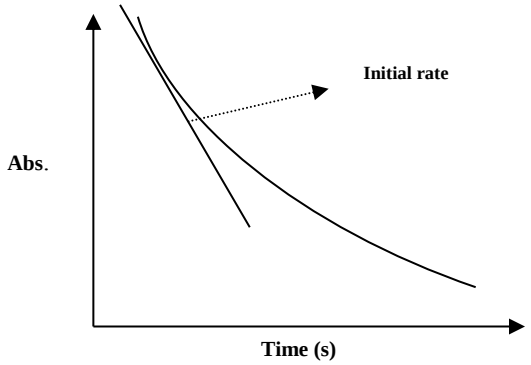

Fig. 1: Determination of the initial rate of the disappearance of ALZ from an absorbance vs. time plot.

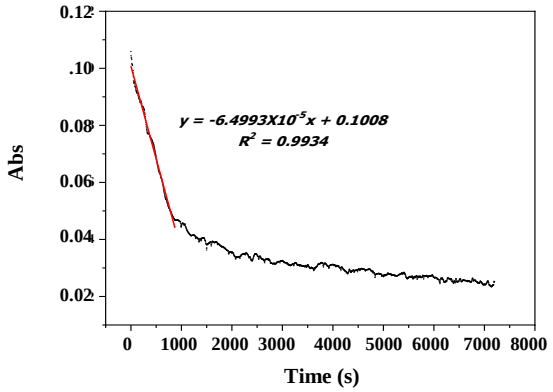

Fig. 2: The UV-Vis kinetics of the hydrolysis of ALZ in the basic medium at 25°C. 2.0 mL of 2.00 × 10^{-5} M ALZ and 1.0 mL of 0.1 M NaOH.

the disappearance of ALZ can be obtained by fitting the first part of the abs. vs. time graph to a least-square linear relationship. As shown in Fig. 2, the initial rate of this experimental run equals the negative value of the slope (6.499×10^{-5} M/s).

The order of Reaction (8) can be verified by the method of initial rates. Further rates were obtained at different concentrations of ALZ by changing the ALZ/OH^- volume ratio but keeping the total reaction volume at 3.0 mL. A complete summary of the kinetic experiments at 25°C are shown in Table 1, where the standard deviation for the logarithmic values of the rate was calculated according to the following relationship [31]:

$$\text{For} \quad y = \log x \quad \Rightarrow \quad STD_y = 0.434 \frac{STDx}{x} \qquad (11)$$

Table 1: Summary of the kinetic experiments for reaction (8) at 25°C.

[ALZ]/mol.L^{-1}		0.0012	0.0006	0.0004	0.0003	0.00024
log [ALZ]		-2.92	-3.22	-3.4	-3.52	-3.62
Initial Rate/M s^{-1}	Trial 1	1.12×10^{-5}	2.07×10^{-6}	2.83×10^{-6}	3.03×10^{-6}	1.82×10^{-6}
	Trial 2	8.57×10^{-5}	8.91×10^{-5}	4.60×10^{-6}	3.63×10^{-6}	5.35×10^{-6}
	Trial 3	2.60×10^{-6}	1.10×10^{-6}	3.50×10^{-6}	5.43×10^{-7}	6.47×10^{-7}
log (initial rate)	Trial 1	-4.95	-5.68	-5.55	-5.52	-5.74
	Trial 2	-4.07	-4.05	-5.34	-5.44	-5.27
	Trial 3	-5.59	-5.96	-5.46	-6.27	-6.19
Ave. (initial rate)/M s^{-1}		3.3167×10^{-5}	3.0757×10^{-5}	3.6433×10^{-6}	2.4010×10^{-6}	2.6057×10^{-6}
STD (initial rate)		4.5698×10^{-5}	5.0529×10^{-5}	8.9366×10^{-7}	1.6368×10^{-6}	2.4480×10^{-6}
Ave. log (initial rate)		-4.87	-5.23	-5.45	-5.74	-5.73
STD log (initial rate)		0.60	0.71	0.11	0.30	0.41

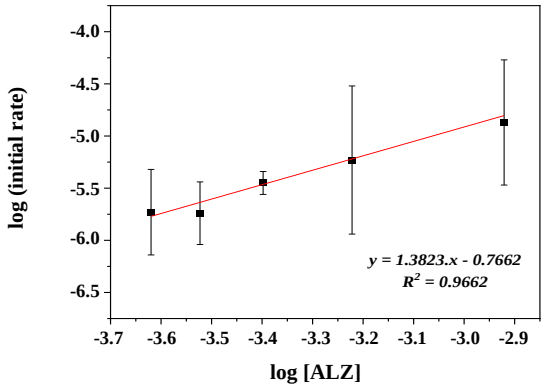

Fig. 3: Determination of the order of reaction (8) at 25°C by the method of initial rates. [OH⁻] = 0.1 M.

Fig. 3 shows the linear relationship between log (initial rate) vs. log [ALZ]. The error bars in the graph represent the standard deviation obtained from three kinetics trials. By applying Eq. (9), the order of reaction (8) should equal the slope of the graph, which is equal to 1.3823. This value is close to unity, which is what is expected from the assumption of this study, by keeping [OH$^-$] in excess, leaving a pseudo-first-order reaction in respect to [ALZ].

The apparent pseudo-first-order rate constant of this reaction can also be determined from the intercept of Fig. 3 according to Eq. (9). This gives a value of k'=0.1713 s^{-1} and the rate law for the reaction (8) is now:

$$\text{Rate} = 0.1713[\text{ALZ}]^{1.3823} \qquad (12)$$

Recall that value of $k' = k_r$ [OH$^-$]. Thus, for a concentration of 0.1 M of OH$^-$, the bimolecular rate constant k_r is estimated at 1.71 M^{-1} s^{-1}. This value reflects the high speed of the hydrolysis of Alizarin in the basic medium.

Effect of temperature

The effect of temperature on the rate of reaction (8) was studied in the range of 25-50° C at 5°C intervals. The study was done using a fixed concentration of the dye (2.00×10^{-5} M) and NaOH (0.1 M). Each experiment was repeated three times in order to obtain accurate results. The initial rates and the pseudo-first-order rate constants (k') were determined as explained earlier and using the pre-determined value of the reaction order of 1.3823. The results of this study are tabulated in Table 2. The standard deviation for the natural logarithm of ln k' was calculated according to the following equation [31]:

$$\text{For} \quad y = \ln x \quad \Rightarrow \quad STD_y = \frac{STD_x}{x} \qquad (13)$$

Fig. 4 shows an Arrhenius plot for ln k' vs. 1/T (in units of K^{-1}) for the data obtained in this work. The data fit well to linear regression with R^2 close to unity (0.9968). Strangely, the graph shows an anti-Arrhenius behavior with a positive slope (+12032.94 K^{-1}). This infers that the apparent activation energy for Reaction (8) under our experimental conditions is negative. Using the value of the slope and the universal gas constant (R), E_a can be determined

Table 2. Effect of temperature on the rate of reaction (1) at constant ALZ concentration of 2.0 × 10^{-5} M) and 0.1 M NaOH.

			Trial 1			Trial 2			Trial 3				
Temp.(C°)	Temp. (K)	1/T (K^{-1})	Initial Rate/M s^{-1}	k' (s^{-1})	ln k'	Initial Rate/M s^{-1}	k' (s^{-1})	ln k'	Initial Rate/M s^{-1}	k' (s^{-1})	ln k'	ln k' (ave.)	STD (lnk')
25	298.15	3.35×10^{-3}	1.186×10^{-5}	37.102	3.614	1.201×10^{-5}	37.584	3.627	1.543×10^{-5}	48.275	3.877	3.706	0.040
30	303.15	3.30×10^{-3}	8.794×10^{-6}	27.516	3.315	7.193×10^{-6}	22.507	3.114	4.513×10^{-6}	14.121	2.648	3.025	0.113
35	308.15	3.25×10^{-3}	3.321×10^{-6}	10.390	2.341	8.485×10^{-6}	26.550	3.279	2.542×10^{-6}	7.952	2.073	2.564	0.247
40	313.15	3.19×10^{-3}	1.627×10^{-6}	5.091	1.627	1.844×10^{-6}	5.771	1.753	1.799×10^{-6}	5.630	1.728	1.703	0.039
45	318.15	3.14×10^{-3}	1.089×10^{-6}	3.408	1.226	1.173×10^{-6}	3.670	1.300	1.030×10^{-6}	3.223	1.170	1.232	0.053
50	323.15	3.09×10^{-3}	3.587×10^{-7}	1.122	0.115	7.740×10^{-7}	2.422	0.884	7.504×10^{-7}	2.348	0.854	0.618	0.705

to be -100.04 kJ/mol (*i.e.*, -23.91 kcal/mol). Negative E_a values are not very common in the chemical literature. However, they were observed for some reactions, particularly those involving $OH^{\bullet}$ radicals [23-25,39]. For instance, in a theoretical study to study OH addition to ethenes, E_a values were determined to be in the range of +3.37 to -4.45 kcal/mol, depending on substituted ethene structure [39]. In the case of the addition of OH to toluene, *Suh et al.*, have calculated the E_a value at a different level of theories and found them to be in the range of -1.5 to – 3.5 kcal/mol, depending on the position of attack on the toluene and the basis set used. The high magnitude of the E_a for ALZ + OH^- determined in our work compared to those of OH radicals' additions is an indication of the speed of the hydroxide addition to ALZ, and phenols in general.

In their 2013 paper, Revell and Williamson provided an interpretation for reactions involving negative activation energy [21]. Since an elementary step should proceed (by definition) in a single step, with "an inherently positive activation energy" [21], the authors suggested that anti-Arrhenius reaction should have a complex mechanism involving a rapid equilibrium with an intermediate C, before forming the final product/s, as discussed earlier by Eq. (2). According to the authors, the apparent activation energy is related to enthalpies of steps 1 and 2 as per the following relationship [21]:

$$E_a = E_2 + \Delta H_1 \quad (14)$$

where ΔH_1 is the enthalpy change between the reactant pair (A+B) and the intermediate C, and E_2 is the activation barrier between C and P.

Later in this paper, an interpretation for the negative E_a value obtained in this work will be provided based on our *ab-initio* calculations. The theoretical study also reveals the formation of the proposed intermediate C.

Effect of ionic strength

The ionic strength of the solution does not only affect the rate of ion-containing reactions but also can reveal valuable information on the nature of the ions involved. According to the model presented by *Brönsted* and *Bjerrum*, the rate of an ionic reaction depends on the ionic strength as per the following expression [40,27]:

$$\log k = \log k_0 + 2AZ_A Z_B \sqrt{I} \quad (15)$$

Where k_0 is the rate constant at infinite dilution, I is the ionic strength of the solution, Z_A, and Z_B are the ion charges, and A is a constant that equals 0.51 $mol^{-½}$ $dm^{3/2}$ at 25 Cº. According to this expression, better known as the 'kinetic salt effect', increasing the ionic strength increases the rate constant for reactions between ions of the same charge, and decreases the rate constant for those having opposite charges [40,27]. Thus, for the sake of this study, studying this effect can reveal if OH^- is truly part of the rate-determining step of the hydrolysis of Alizarin dye.

We investigated the effect of ionic strength on the reaction by carrying out kinetic experiments with five different concentrations of aqueous KCl. Table 3

Table 3. Effect of the ionic strength on the rate of ALZ hydrolysis at constant ALZ concentration of 2.0 × 10^{-5} M) and 0.1 M NaOH.

		Trial 1			Trial 2			Trial 3				
Ionic strength/M	$(I)^{0.5}$/M	Initial rate/s^{-1}	k'/s-1	log k'	Initial rate/s^{-1}	k'/s^{-1}	log k'	Initial rate/s^{-1}	k'/s-1	log k'	log k' (Ave.)	k' (STD)
0.000	0.000	8.543×10^{-5}	267.295	2.427	5.450×10^{-5}	170.523	2.232	3.571×10^{-5}	111.744	2.048	2.236	0.037
0.125	0.354	4.533×10^{-5}	141.841	2.152	2.517×10^{-5}	78.744	1.896	1.817×10^{-5}	56.842	1.755	1.934	0.045
0.250	0.500	6.767×10^{-6}	21.172	1.326	2.917×10^{-5}	91.259	1.960	2.417×10^{-5}	75.615	1.879	1.722	0.087
0.375	0.612	9.167×10^{-6}	28.681	1.458	1.450×10^{-5}	45.368	1.657	2.717×10^{-5}	85.002	1.929	1.681	0.061
0.500	0.707	3.905×10^{-6}	12.218	1.087	4.833×10^{-6}	15.123	1.180	2.250×10^{-5}	70.399	1.848	1.371	0.131

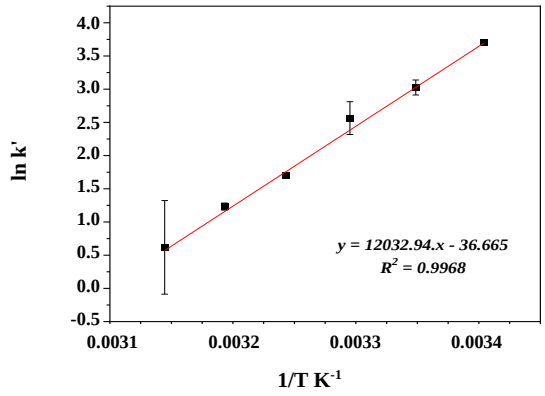

Fig. 4: Arrhenius plot for the hydrolysis of ALZ at a fixed concentration of the dye (2.0 × 10^{-5} M) and 0.1 M NaOH.

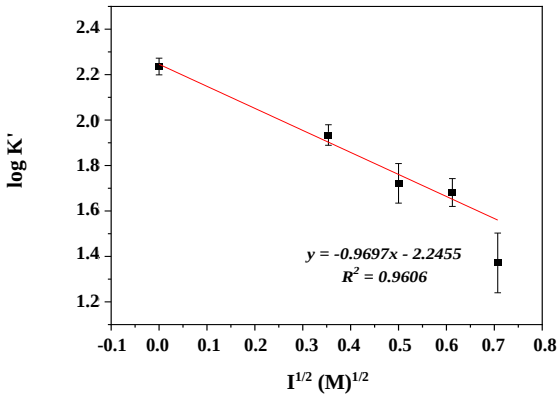

Fig. 5: Effect of the ionic strength on the rate of ALZ hydrolysis. [ALZ] = 2.0 × 10^{-5} M, [NaOH] = 0.1 M. T = 25°C.

summarizes the results of this part of the study. The standard deviation for log *k'* presented in the table was calculated according to Eq. (11). Fig. 5 shows a plot of log *k'* vs. the square root of *I* for five experiments that differ only in the concentration of KCl at 25°C. The error bars in the figure represent the standard deviation of three trials. The data follows a linear regression function with a slope = -0.9697 (R^2 = 0.9606). This result reveals that one of the ions involved in the Rate-Determining Step (RDS) of the reaction mechanism must be single negatively charged. Thus, we conclude that OH^- is indeed part of the RDS.

Interpretation of the experimental results based on ab-initio calculations

In the previous sections, the kinetics for the hydrolysis of ALZ dye in a basic medium was studied. The oddest observation was the negative E_a for the reaction, obtained under the conditions of the study. Also, the effect of the ionic strength on the reaction rate revealed that OH^- must be part of the RDS of the reaction mechanism. In order to comprehend the nature of this reaction, we carried out *ab-initio* calculations on ALZ hydrolysis as explained earlier in the theoretical section.

Fig. 6 shows the optimized structures of the ALZ molecule and its anion, named (I), formed upon an abstraction of one portion from ALZ by OH^- at B3LYP/6-31+G(d,p) level of theory. We attempted to locate a transition state for the first step of this reaction using different basis sets. However, all these attempts have failed. The calculations, though, revealed the formation of an intermediate, named (II), shown also in Fig. 6. This intermediate combines the products ALZ anion (I) and H_2O molecule attached by hydrogen bonding.

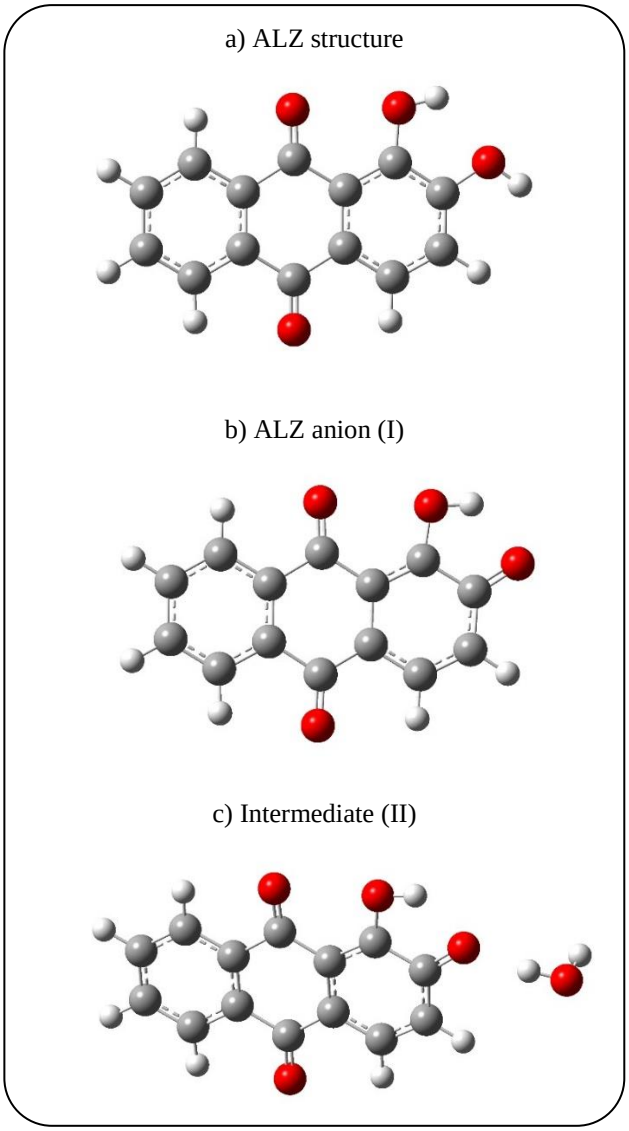

Fig. 6: Optimized structures for a) ALZ dye molecule, b) ALZ anion (I), and c) ALZ-OH$^-$ intermediate (II), obtained at B3LYP/6-31+G(d,p) level of theory. C atom, grey; O atom, red.

In order to confirm the nonexistence of the transition state for the reaction, we explored the potential energy surface for this reaction by scanning the distance between OH^- and the phenolic proton in ALZ at 0.1Å for 30 steps. The Potential Energy Scan (PES), obtained at B3LYP/6-31+G(d,p) /6-31+G(d,p) level of theory, is shown in Fig. 7. It is evident that the addition of OH^- to ALZ proceed smoothly from right to left in the figure without passing any maxima that 'might' correspond to a transition state. In order to confirm this finding, we repeated the calculations using the B97D3 density functional suggested by *Grimme* [35]. Since the hydrolysis of ALZ by OH^- takes place in an aqueous solution, using this function proved to provide better results in similar cases [36,41,42]. Under B97D3/6-31+G(d,p) /6-31+G(d,p) level of theory, a similar PES to Fig. 7 was obtained, confirming no TS exists at this level.

Based on the above results, we propose that Reaction (1) proceeds as follows; the hydroxide anion first approaches the ALZ molecule forming strong H-bonding with the phenolic protons, as seen to the right of Fig. 7. The reaction then continues with no energy barrier forming intermediate II, followed by the slow decomposition of II into anion I and water. This mechanism is in concert with that of Eq. (3).

The relative energies of intermediate II, and the final product (I and H_2O) to those of ALZ are shown in Table 4. The energies were calculated as described earlier in the theoretical part. For the purpose of obtaining accurate energies, the single point energies of all species involved in the table were computed at MP2/6-311+G(d,p) level, after successful optimization at either B3LYP or B97D3 levels. The thermodynamic parameters, enthalpy (ΔH_{298}), and Gibbs free energy at 298K (ΔG_{298}), and entropy (ΔS_{298}) were calculated as described in the theoretical section and Eq. (10).

An energy level diagram, summarizing the theoretical results obtained in this work is shown in Fig. 8. The graph, which is plotted in terms of free Gibbs energies, shows that the formation of intermediate II is highly exergonic (spontaneous) at room temperature. Once it is formed, II can decompose to final products. At MP2/6-311+G(d,p)//B97D3/6-31+G(d,p) level of theory, however, II is more stable than the separated anion I + H_2O pair. Therefore, we expect the products to be in the final form of intermediate II in an aqueous solution.

The computational results, illustrated in Fig. 8, show large differences between the energies obtained at B3LYP and B97D3 levels. By adding dispersion effects through the B97D3 functional, the enthalpy (ΔH_{298}) of the first step has dropped from -85.6 to -40.3 kcal/mol. A similar correlation is observed for the second step. In addition, the theoretical ΔH_{298} values for the 1st step (-40.3 kcal/mol) and for the 2nd step (-34.5 kcal/mol) obtained at B97D3 level are within the range of the experimental E_a value (-23.9 kcal/mol). According to Eq. (14), the apparent E_a can be assumed to be the sum of ΔH_1 and E_2, where the latter is the activation barrier for the last step. Since such barrier

Table 4. Relative energy values for reaction (1) calculated at MP2/6-311+G(d,p)//B3LYP/6-31+G(d,p) and MP2/6-311+G(d,p)//B97D3/6-31+G(d,p) level of theories.

	ALZ + OH^-	ALZ - OH^- intermediate (II)	ALZ anion (I) + Water
MP2/6-311+G(d,p)//B3LYP/6-31+G(d,p)			
ΔH_0 (kcal/mol)	0.0	-85.2	-74.1
ΔH_{298} (kcal/mol)	0.0	-85.6	-74.3
ΔG_{298} (kcal/mol)	0.0	-78.5	-74.6
ΔS_{298} (cal. K/mol)	0.0	-23.9	0.9
MP2/6-311+G(d,p)//B97D3/6-31+G(d,p)			
ΔH_0 (kcal/mol)	0.0	-40.0	-34.4
ΔH_{298} (kcal/mol)	0.0	-40.3	-34.5
ΔG_{298} (kcal/mol)	0.0	-33.2	-34.9
ΔS_{298} (cal. K/mol)	0.0	-23.9	1.6

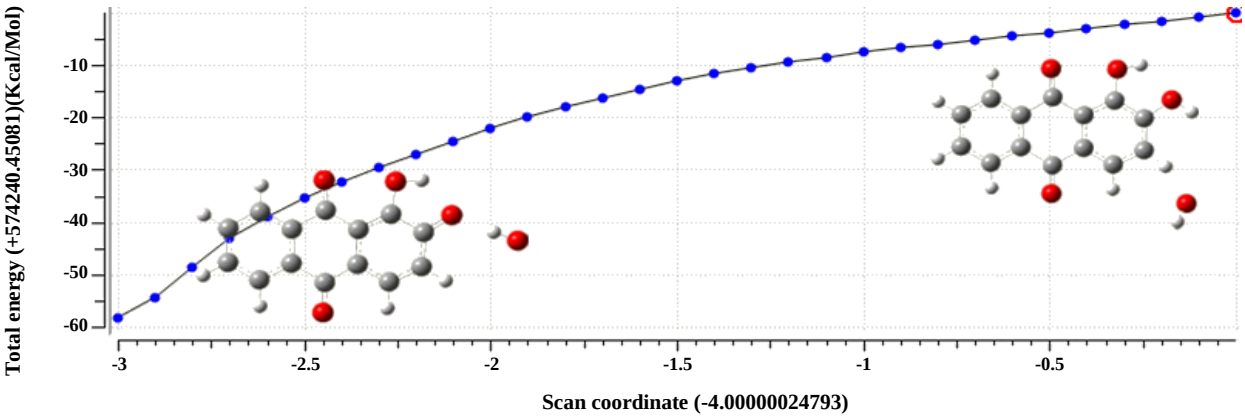

Fig. 7: Potential energy scan (PES) for the addition of OH^- to ALZ obtained at B3LYP/6-31+G(d,p) /6-31+G(d,p) level of theory.

did not exist in our case, it is safe to assume that the apparent E_a is roughly equal to ΔH_1. Consequently, we conclude that the MP2/6-311+G(d,p)//B97D3/6-31+G(d,p) calculation level has provided a good estimation of the negative E_a obtained in this work.

CONCLUSIONS

In this work, the hydrolysis of Alizarin dye (ALZ) in a basic medium was studied. The reaction kinetics was followed by recording the UV-Vis absorbance of the reaction mixture upon injecting a dilute solution of ALZ with an excess amount of NaOH. The initial rates of the reaction at a different convention of the dye were determined from their abs. vs. time plots. Then, the method of initial rates was used to determine the order of the reaction, which was found to be close to unity, in agreement with pseudo-first-order reaction approximation. The effect of temperature on the reaction was studied in the range of 25-50°C. Strangely, the reaction was found to follow an anti-Arrhenius behavior with a positive slope. Thus, the apparent activation energy was found to be -23.91 kcal/mol. A study of the effect of the ionic strength, using different concentrations of KCl, on the reaction rate showed a negative slope. This infers that OH^- is involved in the rate-determining step of the reaction. In order to comprehend these findings, a theoretical study

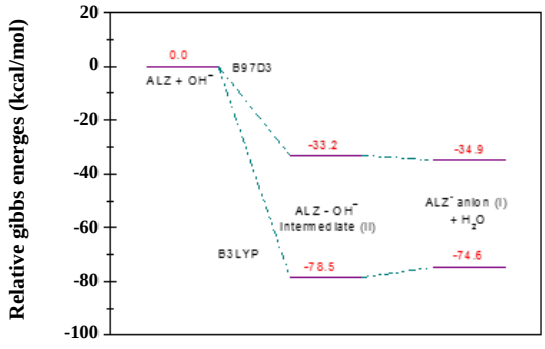

Fig. 8: Potential energy level diagram for the hydrolysis of ALZ at MP2/6-311+G(d,p)//B3LYP/6-31+G(d,p) and MP2/6-311+G(d,p)//B97D3/6-31+G(d,p) level of theories. Energies represent relative Gibbs free energies in kcal/mol at 298 K and 1 atm.

Implementing the density functionals B3LYP and B97D3 was performed. Single point energies of the species involved in the reaction were also computed at a higher MP2 level in order to obtain better results. The *ab-initio* calculations indicated that no transition state exists for the addition OH^- to ALZ. Also, the study revealed the formation of a reaction intermediate that combines ALZ^- anion and water molecule. Thus, a reaction mechanism is suggested based on Eq. (3). The Gibbs free energy for step 1, the formation of intermediate II, was determined to be -33.2 and -78.5 at B97D3 and B3LYP levels, respectively. Since the B97D3 value is closer to the experimental E_a than that of B3LYP, the Grimme's functional proved to better describe aqueous reactions. Also, the standard reaction enthalpy for the overall reaction was determined to be –34.5 kcal/mol, which is in the range of the experimental E_a determined in this work.

The importance reinforces our understanding of the anti-Arrhenius behavior in the hydrolysis of phenolic dyes in a basic medium. Also, the outcomes of this research can be used to better optimize the conditions of the adsorptive removal of those dyes from wastewater resources.

Acknowledgments

The authors are grateful to the Faculty of Science at An-Najah National University and the College of Arts and Sciences at Qatar University for supporting this research. Z. Talie is thankful for the financial support provided by the Middle East Desalination Research Center (MEDRC) fellowship.

Received : Jan. 17, 2020 ; Accepted : May 4, 2020

REFERENCES

[1] World Health Organization, UNICEF, Progress on drinking water, sanitation and hygiene: 2017 Update and SDG baselines. World Health Organization (WHO) and the United Nations Children's Fund (UNICEF), Geneva (2017).

[2] Vörösmarty C.J., McIntyre P.B., Gessner M.O., Dudgeon D., Prusevich A., Green P., Glidden S., Bunn S.E., Sullivan C.A., Liermann C.R., Davies P.M., Global Threats to Human Water Security and River Biodiversity, *Nature*, **467(7315)**:555-561 (2010). doi:10.1038/nature09440

[3] Tong T., Elimelech M., The Global Rise of Zero Liquid Discharge for Wastewater Management: Drivers, Technologies, and Future Directions, *Environ. Sci. Technol.*, **50 (13)**: 6846-6855 (2016). doi:10.1021/acs.est.6b01000

[4] Badran I., Khalaf R., Adsorptive Removal of Alizarin Dye from Wastewater Using Maghemite Nanoadsorbents, *Sep. Sci. Technol.*, **55**:1-16 (2019). doi:10.1080/01496395.2019.1634731

[5] Kant R., Textile Dyeing Industry an Environmental Hazard, *Natural Science*, **4**:22-26 (2011). doi:10.4236/ns.2012.41004.

[6] Mahmoodabadi M., Khoshdast H., Shojaei V., Efficient Dye Removal from Aqueous Solutions Using Rhamnolipid Biosurfactants by Foam Flotation, *Iran. J. Chem. Chem. Eng. (IJCCE)*, **38(4)**: 127-140 (2019).

[7] Kamranifar M., Naghizadeh A., Montmorillonite Nanoparticles in Removal of Textile Dyes from Aqueous Solutions: Study of Kinetics and Thermodynamics, *Iran. J. Chem. Chem. Eng. (IJCCE)*, **36(6)**: 127-137 (2017).

[8] Naghizadeh A., Ghafouri M., Synthesis and Performance Evaluation of Chitosan Prepared from Persian Gulf Shrimp Shell in Removal of Reactive Blue 29 De from Aqueous Solution (Isotherm, Thermodynamic and Kinetic Study), *Iran. J. Chem. Chem. Eng. (IJCCE)*, **36(3)**:25-36 (2017).

[9] Katheresan V., Kansedo J., Lau S.Y., Efficiency of Various Recent Wastewater Dye Removal Methods: A Review, *J. Environ. Chem. Eng.*, **6(4)**: 4676-4697 (2018). doi:10.1016/j.jece.2018.06.060

[10] Shahid ul I., Sun G., Thermodynamics, Kinetics, and Multifunctional Finishing of Textile Materials with Colorants Extracted from Natural Renewable Sources, *ACS Sustainable Chem. Eng.*, **5(9)**: 7451-7466 (2017).
doi:10.1021/acssuschemeng.7b01486

[11] Zulmajdi S.L.N., Zamri N.I.I., Yasin H.M., Kusrini E., Hobley J., Usman A., Comparative Study on the Adsorption, Kinetics, and Thermodynamics of the Photocatalytic Degradation of Six Different Synthetic Dyes on TiO_2 Nanoparticles, *React. Kinet. Mech. Catal* (2019).
doi:10.1007/s11144-019-01701-x

[12] Hossini H., Rezaee A., Rastegar S.O., Hashemi S., Safari M., Equilibrium and Kinetic Studies of Chromium Adsorption from Wastewater by Functionalized Multi-Wall Carbon Nanotubes, *React. Kinet. Mech. Catal.*, **112(2)**: 371-382 (2014).
doi:10.1007/s11144-014-0699-x

[13] Nassar N.N., Marei N.N., Vitale G., Arar L.A., Adsorptive Removal of Dyes from Synthetic and Real Textile Wastewater Using Magnetic Iron Oxide Nanoparticles: Thermodynamic and Mechanistic Insights, *Can. J. Chem. Eng.*, **93(11)**: 1965-1974 (2015).
doi:10.1002/cjce.22315

[14] Alnajjar M., Hethnawi A., Nafie G., Hassan A., Vitale G., Nassar N.N., Silica-Alumina Composite as an Effective Adsorbent for the Removal of Metformin from Water, *J. Environ. Chem. Eng.*, **7(3)**: 102994 (2019).
doi:10.1016/j.jece.2019.102994

[15] Javadnia N., Farrokhnia A., The Thermodynamic and Kinetics Study of Removal of Cd(II) by Nanoparticles of Cobalt Oxide in Aqueous Solution, *Iran. J. Chem. Chem. Eng. (IJCCE)*, **38 (1)**: 127-139 (2019).

[16] Naghizadeh A., Kamranifar M., Yari A.R., Mohammadi M.J., Equilibrium and Kinetics Study of Reactive Dyes Removal from Aqueous Solutions by Bentonite Nanoparticles, *Desalin. Water Trear.*, **97**:329-337 (2017).

[17] Naghizadeh A., Nabizadeh R., Removal of Reactive Blue 29 Dye by Adsorption on Modified Chitosan in The Presence of Hydrogen Peroxide, *Environ. Prot. Eng.*, **42(1)**: 149 - 267 (2016).

[18] Santa Cruz Biotechnology Inc., "Alizarin MSDS" (sc-214519) Santa Cruz, California 95060, USA (2009).

[19] Pirillo S., Ferreira M.L., Rueda E.H., The Effect of pH in the Adsorption of Alizarin and Eriochrome Blue Black R onto Iron Oxides, *J. Hazard. Mater.*, **168(1)**:168-178 (2009).
doi:10.1016/j.jhazmat.2009.02.007

[20] Engel T., Reid P., Engel T., Hehre W., "Physical Chemistry". 3rd ed., Pearson, Boston (2013).

[21] Revell L.E., Williamson B.E., Why Are Some Reactions Slower at Higher Temperatures?, *J. Chem. Educ.*, **90(8)**: 1024-1027 (2013).

[22] Upadhyay S.K., "Chemical Kinetics and Reaction Dynamics", Springer, New Delhi, India (2006).

[23] Chuong B., Stevens P.S., Kinetic Study of the OH + Isoprene and OH + Ethylene Reactions between 2 and 6 Torr and over the Temperature Range 300−423 K, *J. Phys. Chem. A*, **104(22)**: 5230-5237 (2000).
doi:10.1021/jp993613a

[24] Hand M.R., Rodriquez C.F., Williams I.H., Balint-Kurti G.G., Theoretical Estimation of the Activation Energy for the Reaction HO• + H_2O → H_2O + •OH: Importance of Tunneling, *J. Phys. Chem. A*, **102(29)**: 5958-5966 (1998).
doi:10.1021/jp980838x

[25] Suh I., Zhang D., Zhang R., Molina L.T., Molina M.J., Theoretical Study of OH Addition Reaction to Toluene, *Chem. Phys. Lett.*, **364(5)**: 454-462 (2002).
doi:10.1016/S0009-2614(02)01364-7

[26] OriginLab Corporation, "OriginPro 9.1: Scientific Data Analysis and Graphing Software", Northampton, MA, USA (2019).

[27] Atkins P.W., De Paula J., Keeler J., "Atkins' Physical Chemistry". 11th ed., Oxford University Press, Oxford, United Kingdom; New York, NY (2018).

[28] Felix L., Kinetic study of the Discoloration of Crystal Violet Dye in Sodium Hydroxide Medium, *J. Chem. Appl. Chem. Eng.*, **2(1)**:2 (2018).

[29] Fisichella S., Occhipinti S., Alberghina G., Amato M., Kinetics of Hydrolysis of Dichlorotriazinyl Reactive azo Dyes, *Text. Res. J.*, **51(11)**:683-687 (1981).

[30] Badran I., "Hot-Wire Chemical Vapour Deposition Chemistry and Kinetics of New Precursors in the Gas Phase and on the Wire Surface", Ph,D Thesis, Department of Chemistry, of Calgary, Calgary, Alberta, Canada (2014).

[31] Harris D.C., Lucy C.A., "Quantitative Chemical Analysis", 9th ed., W.H. Freeman & Company, New York (2016).

[32] Badran I., Rauk A., Shi Y., New Orbital Symmetry-Allowed Route for Cycloreversion of Silacyclobutane and Its Methyl Derivatives, *J. Phys. Chem. A*, **123 (9)**: 1749-1757 (2019). doi:10.1021/acs.jpca.8b08071

[33] Warad I., Musameh S., Badran I., Nassar N.N., Brandao P., Tavares C.J., Barakat A., Synthesis, Solvatochromism and Crystal Structure of Trans-$[Cu(Et_2NCH_2CH_2NH_2)_2.H_2O](NO_3)_2$ Complex: Experimental with DFT Combination, *J. Mol. Struct.*, **1148**: 328-338 (2017). doi:10.1016/j.molstruc.2017.07.067

[34] Badran I., Rauk A., Shi Y.J., Theoretical Study on the Ring-Opening of 1,3-Disilacyclobutane and H_2 Elimination, *J. Phys. Chem. A*, **116(48)**: 11806-11816 (2012). doi:10.1021/jp3087122

[35] Grimme S., Antony J., Ehrlich S., Krieg H., A Consistent and Accurate *AB Initio* Parametrization of Density Functional Dispersion Correction (DFT-D) for the 94 Elements H-Pu, *J. Chem. Phys.*, **132(15)**: 154104 (2010). doi:10.1063/1.3382344

[36] Manasrah A.D., El-Qanni A., Badran I., Ortega L.C., Perez-Zurita M.J., Nassar N.N., Experimental and Theoretical Studies on Oxy-Cracking of Quinolin-65 as a Model Molecule for Residual Feedstocks, *React. Chem. Eng.*, **2(5)**:703-719 (2017). doi:10.1039/c7re00048k

[37] Frisch M., Trucks G., Schlegel H., Scuseria G., Robb M., Cheeseman J., Scalmani G., Barone V., Petersson G., Nakatsuji H., Gaussian 16. Revision A 3 (2016).

[38] Roy Dennington T., Millam J.M., GaussView, Version 6. Semichem Inc., Shawnee Mission, KS, (2016).

[39] Alvarez-Idaboy J.R., Mora-Diez N., Vivier-Bunge A., A Quantum Chemical and Classical Transition State Theory Explanation of Negative Activation Energies in OH Addition to Substituted Ethenes, *J. Am. Chem. Soc.*, **122 (15)**: 3715-3720 (2000). doi:10.1021/ja993693w

[40] Arnaut L., Formosinho S., Burrows H., Elementary Reactions in Solution. In: Arnaut L, Formosinho S, Burrows H (eds) "Chemical Kinetics", Elsevier, Amsterdam, pp 223-250 (2007). doi:10.1016/B978-044452186-6/50009-2

[41] Grimme S., Ehrlich S., Goerigk L., Effect of the Damping Function in Dispersion Corrected Density Functional Theory, *J. Comput. Chem.*, **32(7)**: 1456-1465 (2011).

[42] Jimenez-Halla J.O.C., Nazemi A., Cundari T.R., DFT Study of Substituent Effects in the Hydroxylation of Methane and Toluene Mediated by an Ethylbenzene Dehydrogenase Active Site Model, *J. Organomet. Chem.* **864**: 44-49 (2018).